

## Supporting Information for

### Highly regioselective complexation of tungsten with $\text{Eu@C}_{82}/\text{Eu@C}_{84}$ : interplay between endohedral and exohedral metallic units induced by electron transfer

Lipiao Bao,<sup>a</sup> Pengyuan Yu,<sup>a</sup> Ying Li,<sup>b</sup> Changwang Pan,<sup>a</sup> Wangqiang Shen,<sup>a</sup> Peng Jin<sup>b,\*</sup> Shuquan Liang<sup>c,\*</sup> and Xing Lu<sup>a,\*</sup>

<sup>a</sup> State Key Laboratory of Materials Processing and Die & Mould Technology, School of Materials Science and Engineering, Huazhong University of Science and Technology, 1037 Luoyu Road, Wuhan, 430074, China. E-mail: [lux@hust.edu.cn](mailto:lux@hust.edu.cn)

<sup>b</sup> School of Materials Science and Engineering, Hebei University of Technology, Tianjin, 300130, China. E-mail: [china.peng.jin@gmail.com](mailto:china.peng.jin@gmail.com)

<sup>c</sup> Department of Materials Science and Engineering, Central South University, Changsha, 410083, China. E-mail: [lsq@csu.edu.cn](mailto:lsq@csu.edu.cn)

**Crystal data of Eu@C<sub>2</sub>(5)-C<sub>82</sub>·Ni(OEP)·2(C<sub>6</sub>H<sub>6</sub>).** black block, 0.20 × 0.20 × 0.17 mm, monoclinic, space group *C2/m*, *a* = 25.236(2) Å, *b* = 15.0375(14) Å, *c* = 19.8277(19) Å,  $\beta$  = 94.3850(10)°, *V* = 7502.3(12) Å<sup>3</sup>, *F*<sub>w</sub> = 1884.45,  $\lambda$  = 0.65250 Å, *Z* = 4, *D*<sub>calc</sub> = 1.668 Mg m<sup>-3</sup>,  $\mu$  = 0.913 mm<sup>-1</sup>, *T* = 100 K, *R*<sub>1</sub>[8461 reflections with *I* > 2σ(*I*)] = 0.0873, *wR*<sub>2</sub> (all 62921 data) = 0.2663, GOF (on *F*<sup>2</sup>) = 1.036. The maximum residual electron density is 1.480 eÅ<sup>-3</sup>. Crystallographic data has been deposited in the Cambridge Crystallographic Data Center (CCDC number: 1579794).

**Crystal data of Eu@C<sub>2</sub>(13)-C<sub>84</sub>·Ni(OEP)·1.61(C<sub>6</sub>H<sub>6</sub>)·0.39(CS<sub>2</sub>).** black block, 0.30 × 0.24 × 0.24 mm, monoclinic, space group *C2/m*, *a* = 25.3346(8) Å, *b* = 15.1339(5) Å, *c* = 19.9751(6) Å,  $\beta$  = 95.6590(10)°, *V* = 7621.4(4) Å<sup>3</sup>, *F*<sub>w</sub> = 1907.70,  $\lambda$  = 0.65250 Å, *Z* = 4, *D*<sub>calc</sub> = 1.663 Mg m<sup>-3</sup>,  $\mu$  = 0.915 mm<sup>-1</sup>, *T* = 100 K, *R*<sub>1</sub>[8432 reflections with *I* > 2σ(*I*)] = 0.0795, *wR*<sub>2</sub> (all 58740 data) = 0.2028, GOF (on *F*<sup>2</sup>) = 1.021. The maximum residual electron density is 1.789 eÅ<sup>-3</sup>. Crystallographic data has been deposited in the Cambridge Crystallographic Data Center (CCDC number: 1851767).

**Crystal data of 2a·CS<sub>2</sub>.** black plate, 0.30 × 0.20 × 0.04 mm, monoclinic, space group *P2<sub>1</sub>/n*, *a* = 22.367(2) Å, *b* = 11.2378(10) Å, *c* = 27.520(3) Å,  $\beta$  = 112.0420(10)°, *V* = 6411.8(10) Å<sup>3</sup>, *F*<sub>w</sub> = 1879.17,  $\lambda$  = 0.65250 Å, *Z* = 4, *D*<sub>calc</sub> = 1.947 Mg m<sup>-3</sup>,  $\mu$  = 2.343 mm<sup>-1</sup>, *T* = 100 K, *R*<sub>1</sub>[15400 reflections with *I* > 2σ(*I*)] = 0.0448, *wR*<sub>2</sub> (all 111667 data) = 0.1248, GOF (on *F*<sup>2</sup>) = 1.042. The maximum residual electron density is 2.677 eÅ<sup>-3</sup>. Crystallographic data has been deposited in the Cambridge Crystallographic Data Center (CCDC number: 1579799).

**Crystal data of 2b·CS<sub>2</sub>.** black plate, 0.10 × 0.08 × 0.02 mm, monoclinic, space group *P2<sub>1</sub>/n*, *a* = 22.3565(8) Å, *b* = 11.4569(4) Å, *c* = 27.6560(10) Å,  $\beta$  = 112.8190(10)°, *V* = 6529.3(4) Å<sup>3</sup>, *F*<sub>w</sub> = 1903.20,  $\lambda$  = 0.65250 Å, *Z* = 4, *D*<sub>calc</sub> = 1.936 Mg m<sup>-3</sup>,  $\mu$  = 2.302 mm<sup>-1</sup>, *T* = 100 K, *R*<sub>1</sub>[13446 reflections with *I* > 2σ(*I*)] = 0.0592, *wR*<sub>2</sub> (all 96159 data) = 0.1609, GOF (on *F*<sup>2</sup>) = 1.062. The maximum residual electron density is 2.563 eÅ<sup>-3</sup>. Crystallographic data has been deposited in the Cambridge Crystallographic Data Center (CCDC number: 1579800).

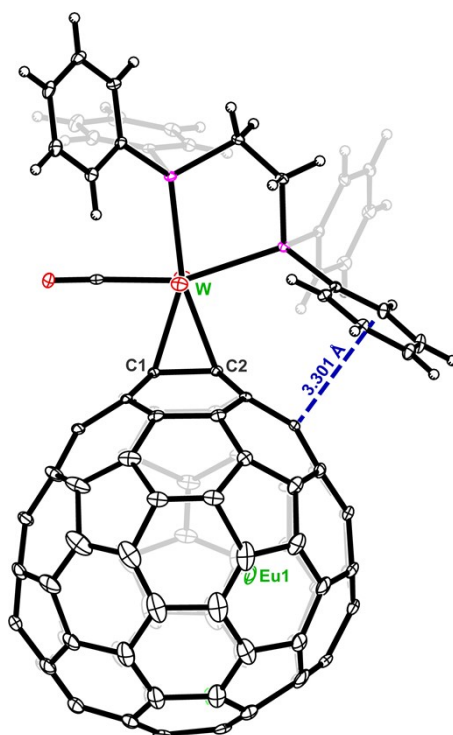


**Fig. S1.** Ortep drawing of **2a** with thermal ellipsoids set at the 20% probability level. Only one cage orientation and the major metal sites are shown. Solvent molecules and the minor metal sites are omitted for clarity.

**Table S1.** The experimentally observed and calculated POAV values of C1 and C2 and the bond lengths of C1-C2 (the site of addition) in  $\text{Eu}@C_2(5)\text{-C}_{82}$ , **2a**,  $\text{Eu}@C_2(13)\text{-C}_{84}$  and **2b**.

	POAV angles ( $^\circ$ )				C1-C2 bond length ( $\text{\AA}$ )	
	C1 <sub>exp</sub>	C1 <sub>cal</sub>	C2 <sub>exp</sub>	C2 <sub>cal</sub>	Experimental	Calculated
$\text{Eu}@C_2(5)\text{-C}_{82}$	10.65	11.60	10.66	11.40	1.36(2)	1.38
<b>2a</b>	15.10	15.80	15.99	15.90	1.47(6)	1.48
$\text{Eu}@C_2(13)\text{-C}_{84}$	11.44	11.70	9.31	11.50	1.38(2)	1.37
<b>2b</b>	15.40	15.50	16.83	16.40	1.49(1)	1.47

**Table S2.** Natural Population Analysis (NPA) Charges and Natural Electron Configuration Populations of the Eu Atom in  $\text{Eu}@C_2(5)\text{-C}_{82}$ , **2a**,  $\text{Eu}@C_2(13)\text{-C}_{84}$  and **2b**.

species	Charge (e)	population
$\text{Eu}@C_2(5)\text{-C}_{82}$	1.41	$6s^{0.06}4f^{7.00}5d^{0.38}6p^{0.13}6d^{0.02}7p^{0.01}$
<b>2a</b>	1.42	$6s^{0.06}4f^{7.00}5d^{0.37}6p^{0.13}6d^{0.02}7p^{0.01}$
$\text{Eu}@C_2(13)\text{-C}_{84}$	1.41	$6s^{0.06}4f^{7.00}5d^{0.37}6p^{0.13}6d^{0.02}7p^{0.01}$
<b>2b</b>	1.42	$6s^{0.06}4f^{7.00}5d^{0.37}6p^{0.13}6d^{0.02}7p^{0.01}$

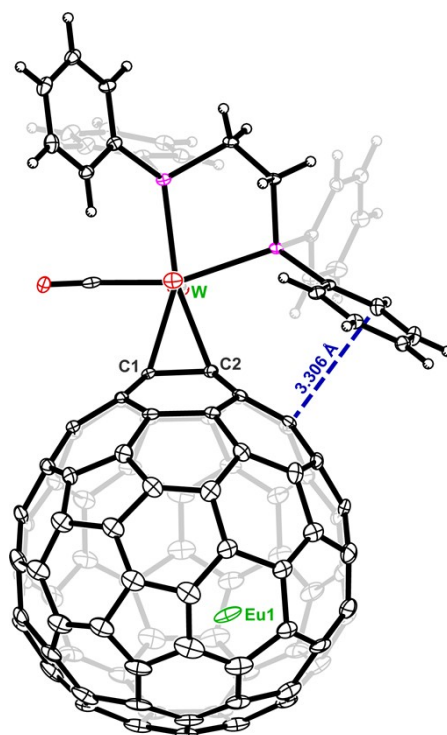


**Fig. S2.** Ortep drawing of **2b** with thermal ellipsoids set at the 20% probability level. Only one cage orientation and the major metal sites are shown. Solvent molecules and the minor metal sites are omitted for clarity.

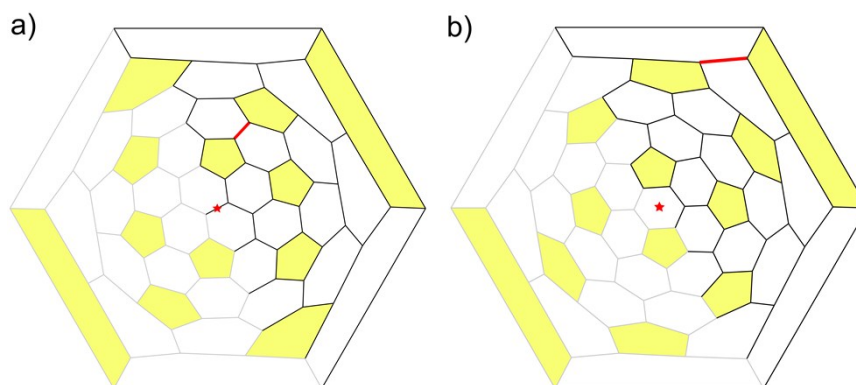


**Fig. S3.** Schlegel diagrams showing a) 62 nonequivalent C-C bonds on  $C_2(5)$ - $C_{82}$  and b) 63 nonequivalent C-C bonds on  $C_2(13)$ - $C_{84}$ . The C-C bonds and pentagons at equivalent sites are displayed in light color. The C-C bonds at the site of addition are highlighted in red. The pentagons are highlighted in yellow. The red star in each diagram indicates the position of the  $C_2$  axis which is perpendicular to the paper plane.

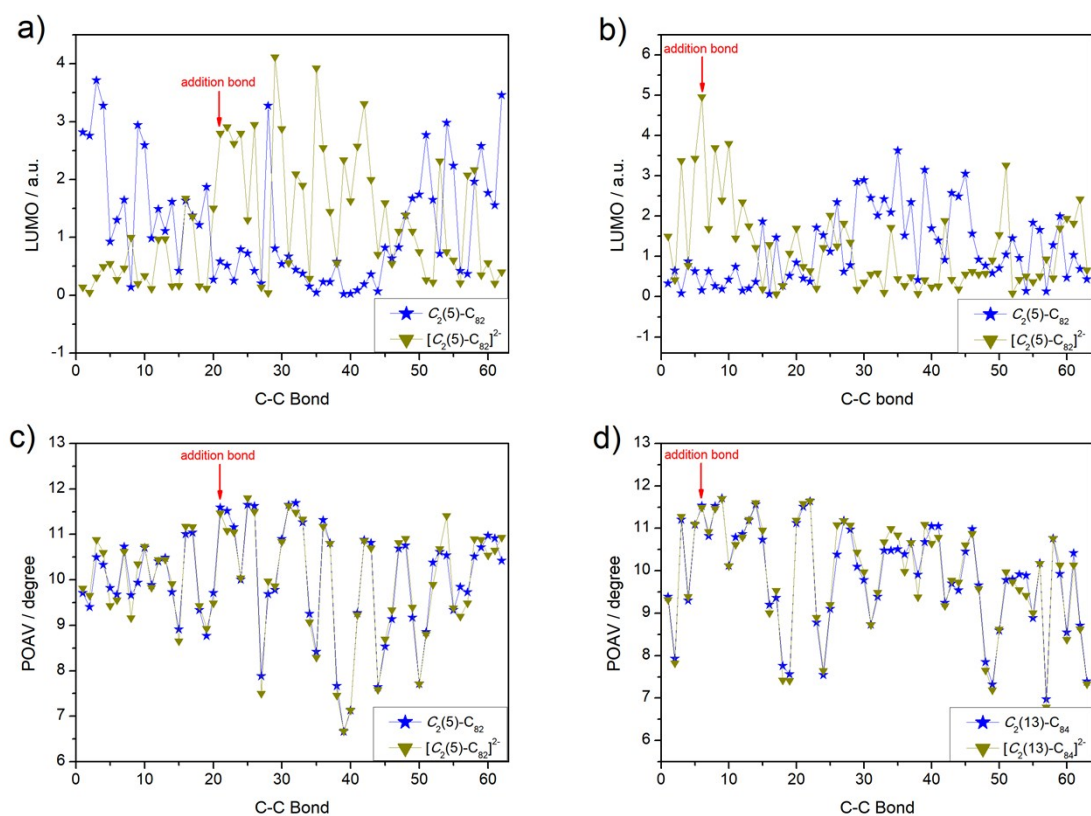


**Fig. S4.** The average LUMO distributions of two bonded cage carbons on a) neutral and di-anionic  $C_2(5)-C_{82}$  and b) neutral and di-anionic  $C_2(13)-C_{84}$ . The average  $\pi$ -orbital axis vector (POAV) values of two bonded cage carbons on c) neutral and di-anionic  $C_2(5)-C_{82}$  and d) neutral and di-anionic  $C_2(13)-C_{84}$ . The bonds at the site of coordination reaction are marked with red arrows. Equivalent C-C bonds on the cage are omitted according to cage symmetry.

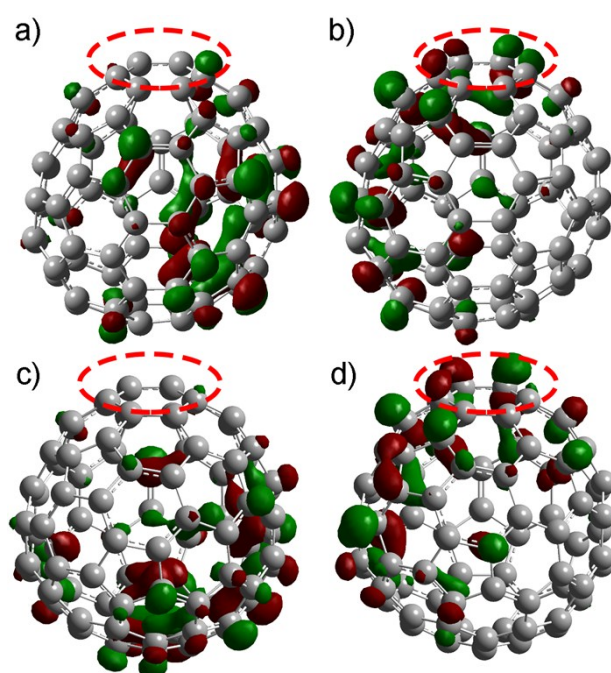


**Fig. S5.** LUMO distributions of a)  $C_2(5)-C_{82}$ , b)  $[C_2(5)-C_{82}]^{2-}$ , c)  $C_2(13)-C_{84}$  and d)  $[C_2(13)-C_{84}]^{2-}$ . The sites of addition are highlighted by red dashed circles.

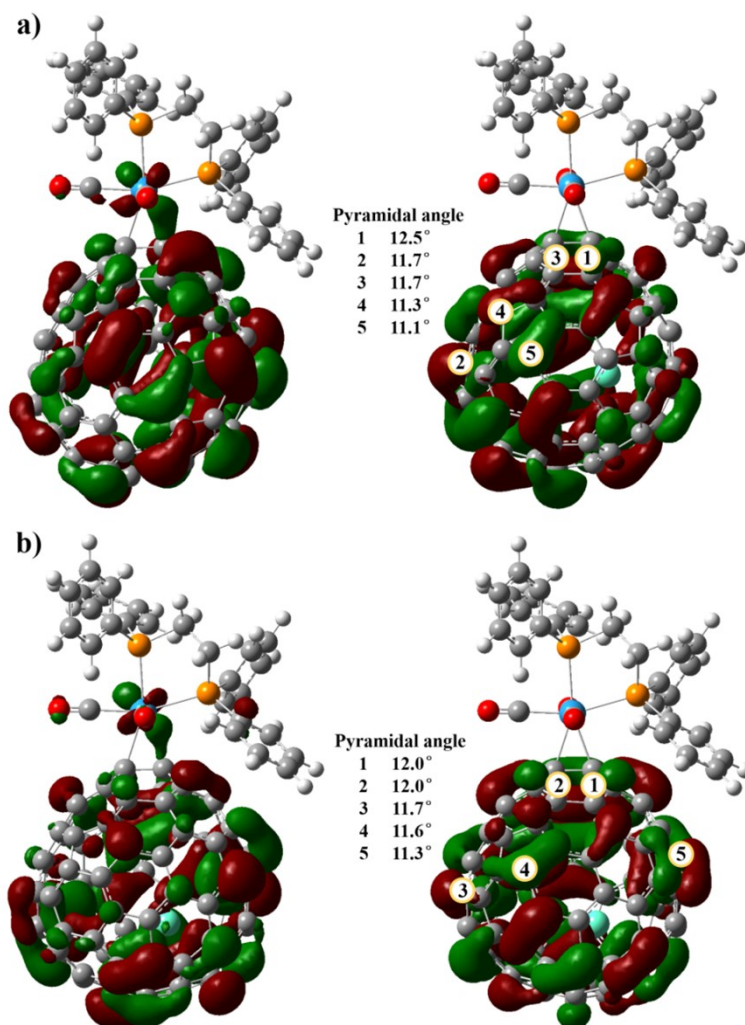


**Fig. S6.** HOMO (left) and LUMO (right) plots of a) **2a** and b) **2b**. The five carbon sites holding both large LUMO distributions and high POAV values are labeled.

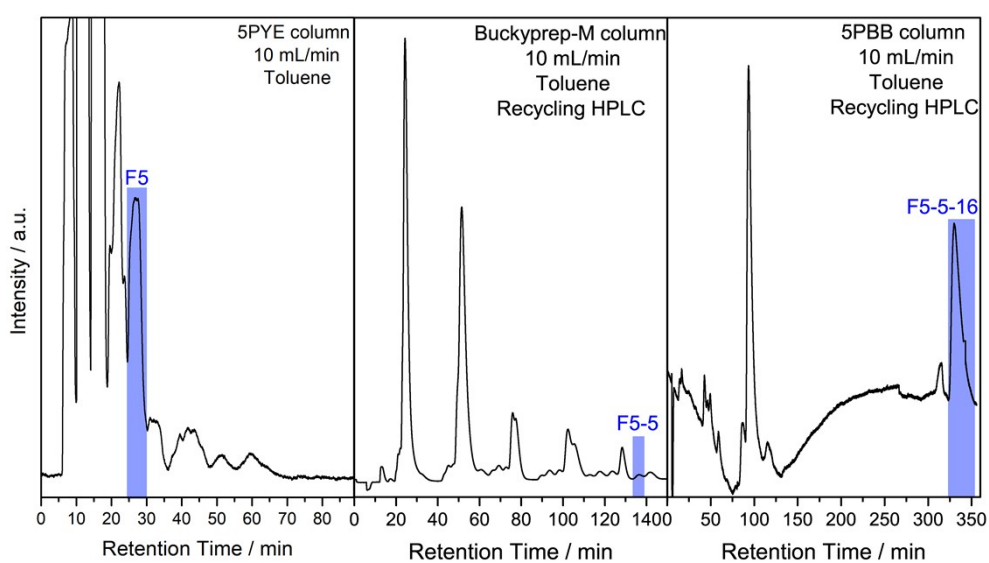


**Fig. S7.** Multi-stage preparative HPLC profiles of the separations of  $\text{Eu}@C_2(5)-C_{82}$ . HPLC conditions: toluene flow; 40 °C; 330 nm detection wavelength.